ABTEILUNG FÜR NEPHROLOGIE DER II. MEDIZINISCHEN KLINIK DER
TECHNISCHEN UNIVERSITÄT MÜNCHEN KLINIKUM RECHTS DER ISAR
(LEITER: UNIV.-PROF. DR. U. HEEMANN)

Everolimus Treatment and Apoptosis in Chronic Allograft Nephropathy (CAN)

Ruiyan Lu

Vollständiger Abdruck der von der Fakultät für Medizin der Technischen Universität München zur Erlangung des akademischen Grades eines Doktors der Medizin genehmigten Dissertation.

Vorsitzender: Univ.-Prof. Dr. D. Neumeier

Prüfer der Dissertation: 1. Univ.-Prof. Dr. U. Heemann

2. Priv.-Doz. Dr. M. J. Stangl

Die Dissertation wurde am 25.11.2003 bei der Technischen Universität München eingereicht und durch die Fakultät für Medizin am 17.03.2004 angenommen.

Contents

1. Abbreviations

ABC	Streptavidin-biotin conjugated peroxidase
APAAP	Alkaline phosphatase anti-alkaline phosphatase
Apaf-1	Apoptotic protease activating factor-1
CAN	Chronic allograft nephropathy
Caspase	Cysteinyl aspartatic acid protease
DAB	3, 3'-diaminobenzidine
DISC	Death inducing signalling complex
FADD	Fas-associated death domain protein
H. E.	Hematoxylin and Eosin
ICE	Interleukin-1ß converting enzyme
IFN-γ	Interferon-γ
IL-1ß	Interleukin-1ß
PAS	Periodic acid-schiff
PBS	Phosphate buffered saline
PCNA	Proliferation cellular nuclear antigen
PDGF	Platelet derived growth factor
PS	Phosphatidylserine
RPA	RNase protection assay
RT-PCR	Reverse transcription polymerase chain reaction
TGF-ß	Transforming growth factor-ß
TNF	Tumor necrosis factor
TNF-R	Tumor necrosis factor receptor
TOR	Target of rapamycin
TUNEL	Terminal deoxynucleotidyl transferase-mediated dUTP nick end labelling

2. Introduction

In 1954, the first successful kidney transplantation in human was performed from one twin to another. Since then it gradually developed to the treatment of choice for patients with end-stage renal disease. One year graft survival has improved during recent years due to better immunosuppressive protocols, namely the use of cyclosporine A, and an improved follow-up of the patients after transplantation (45). However long-term allograft survival was not prolonged remarkably (45).

Chronic allograft nephropathy (CAN) and death of the patient with a functioning graft are the most important causes of long-term graft loss. CAN is clinically characterized by a progressive graft dysfunction with decreasing creatinine clearance and increasing proteinuria which is not related to calcineurin inhibitor toxicity and recurrent or de novo renal disease (37). Histologically it is characterized by a non-specific picture consisting of glomerulopathy, vasculopathy, interstitial fibrosis, and tubular atrophy (23). Both alloantigen-dependent (histoincompatibility, anti-donor specific antibodies, number of acute episodes) and alloantigen-independent factors (ischemia / reperfusion injury, age, gender, lipid abnormalities, and hypertension) are involved in the pathogenesis of CAN (20).

A variety of growth factors, such as transforming growth factor-ß (TGF-ß), and platelet derived growth factor (PDGF)-A and –B contribute to the interstitial fibrosis in progressive CAN (44). They are released by activated macrophages, T lymphocytes, and endothelial cells, promote mesangial cells and fibroblasts, and result in enhanced extracellular matrix synthesis as well as arterial intimal hyperplasia and fibrosis.

There is still no effective treatment to inhibit or prevent CAN. Recently everolimus was found to be a potent immunosuppressive agent. It not only inhibits the proliferation of immune but also that of non-immune cells (41). Interestingly, the tissue remodelling process which occurs during CAN is associated with an increased number of activated and

proliferating cells. Therefore everolimus could induce apoptosis of activated cells, thus clearing them from the graft resulting in an interruption of the remodelling process with improved graft function and long-term outcome.

2.1 Apoptosis and kidney transplantation

2.1.1 Apoptosis and apoptotic pathway

Apoptosis was first described by Kerr et al. in 1972, and is morphologically characterized by cellular blebbing, chromatin condensation, nuclear fragmentation, loss of cell-cell contact, and cell shrinkage. Apoptosis leads to an internucleosomal cleavage of DNA (7), translocation of phosphatidylserine (PS) to the external surface of the cell membrane (32), and proteolytic cleavage of intracellular structural proteins eventually leading to a loss of cell integrity and cell death (31). It is an active, energy consuming process which participates in the regulation of cell number and proliferation.

Two of the key signalling pathways of apoptosis are the death receptor pathway and the mitochondria pathway (15) (Figure 1).

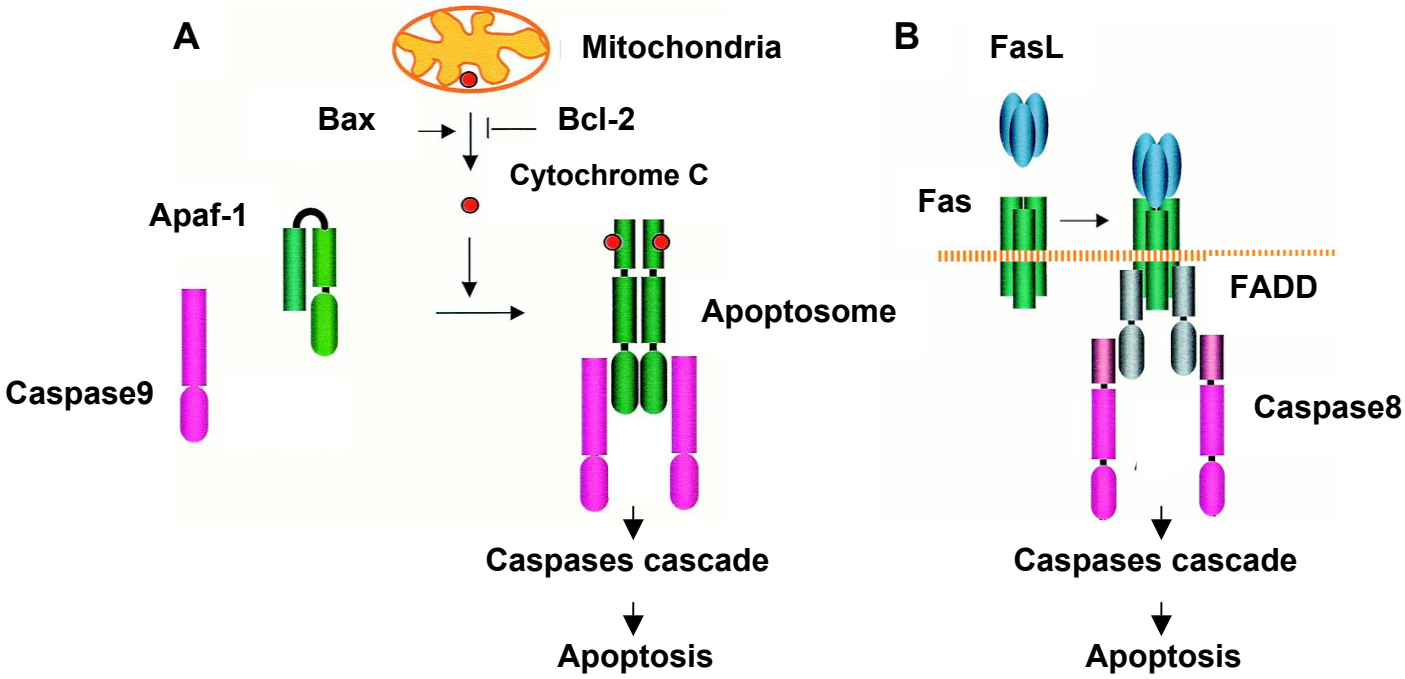

Figure 1. Apoptosis pathways. (**A**) Mitochondria pathway; (**B**) Fas /FasL pathway.

Receptor mediated apoptosis can occur after binding of the respective ligand (FasL, TNF) to the Fas- or TNF- receptor. The Fas receptor (also called Apo-1 or CD95) is a death domain-containing member of the tumor necrosis factor receptor (TNF-R) superfamily (3). Its expression can be upregulated by cytokines, such as tumor necrosis factor (TNF) and interferon-γ (IFN-γ) on various cells such as lymphocytes and tubular cells (48, 15). After binding of FasL to Fas receptor, death inducing signalling complex (DISC) is formed. It activates the procaspase-8 which in turn activates caspase-3 and other caspases in a cascade like fashion (22, 49).

The cysteinyl aspartatic acid proteases (caspases) play a critical role in the execution phase of apoptosis and are responsible for many biochemical and morphological changes associated with apoptosis (2). 14 caspases have been identified so far, which all share a similar structure and substrate specificity. They are divided into inflammatory caspases, such as Caspase-1; and executioner caspases, such as Caspase-3, -6, and -7 (35).

Interleukin-1ß converting enzyme (ICE; Caspase-1) is linking apoptosis and inflammation as it cleaves interleukin-1ß (IL-1ß) which is a potent inflammatory mediator from a pro-form (52).

Caspase-3 is of pivotal importance in the caspase cascade as it is the one ultimately responsible for the majority of the apoptotic effects, although it is supported by two others, Caspase-6 and -7. Together, these three executioner caspases cause the apoptotic phenotype by cleavage or degradation of several important substrates, such as the high-and low-molecular weight DNA-fragmentation and the externalization of PS during apoptosis (29, 30).

The mitochondria pathway induces apoptosis via the release of cytochrome C that forms together with the apoptotic protease activating factor-1 (Apaf-1) and procaspase-9 a complex molecule called ‘apoptosome’ in the cytoplasm. As a result caspase-9 and caspase-3 are activated which initiate the final pathway of apoptosis (52). The release of cytochrome C is

regulated by members of the Bcl-2 family. This family was first discovered in follicular B-cell lymphoma. Among the 19 identified members, Bcl-2 and Bax seem to be of particular importance for the regulation of apoptosis. Bcl-2 has apoptosis inhibiting and Bax has apoptosis promoting properties (53). Bax molecules can associate to homodimers, thus forming channels resulting in the translocation of cytochrome C into the cytosol. Bcl-2 inhibits the formation of these channels through binding to Bax and form Bcl-2-Bax heterodimers (1). Thus it depends on the ratio between Bcl-2 and Bax whether apoptosis is induced or inhibited.

2.1.2 Apoptosis and kidney transplantation

Under physiological conditions apoptosis participates in tissue homeostasis as it counteracts cell proliferation. This is also of pivotal importance during embryogenesis and organogenesis. However, apoptosis might also be involved in acute rejection of renal transplantation and CAN (18, 25, 50). Furthermore, apoptosis occurs during reperfusion in human renal allograft from cadaveric donors (6).

Although the role of apoptosis during rejection of kidney grafts is still debated, it appears likely that apoptosis plays a role in the pathogenesis of acute rejection and CAN as a shift towards the expression of the pro-apoptotic Bax protein with respect to a expression of Bcl-2 protein has been observed in renal tubuli with acute rejection and CAN as compared to normal functioning allograft (8, 34, 36).

2.2 Everolimus in kidney transplantation

The rapamycin derivate 40-O-(2-hydroxyethyl) - rapamycin (everolimus) is a new, orally applicable macrolide immunosuppressive agent (41).

It efficiently prevents graft rejection in animal models of chronic renal allograft rejection (46). Everolimus and rapamycin bind to a cytosolic protein called target of rapamycin (TOR). Everolimus inhibits cell-cycle progression from G1 to S phase by blocking IL-2 receptor and CD28-dependent signalling pathways (4, 42). This effect is not restricted to immune cells, but also affects non-immune cells such as fibroblasts and smooth muscle cells (19, 42). Furthermore, everolimus can induce apoptosis of activated non-immune cells, such as rheumatoid synovial cells, rhabdosarcoma cells and promyelocytic leukemia cell line (21, 33, 43).

Hypercholesterolemia and hypertriglyceridaemia have been observed in clinical studies of everolimus in renal transplant patients. Such lipid abnormalities are treated by diet and CSE-inhibitors. However only little is known about long term effects (5).

2.3 Study aims

Until now, the relationship between apoptosis and everolimus in CAN has been unclear. The present study investigated:

- Whether everolimus could ameliorate CAN even the treatment was delayed;
- Whether everolimus could affect the number of apoptotic cells in CAN and how apoptosis regulating factors were affected;
- What the effects were on cell proliferation in the graft;
- How it affected the growth factor mRNA expression.

3. Materials and Methods

3.1 Animals

Naive inbred male Fisher (F344, RT^{1v1}) and male Lewis (LEW, RT^{1}) rats (Charles River, Sulzfeld, Germany), weighing 170-210 g, were kept under standard conditions and fed with rat chow and water ad libitum. All experiments were approved by a governmental committee on animal welfare.

3.2 Kidney transplantation and model development

A well-established model of CAN was used throughout the experiments (44). Kidneys of Fisher rats were orthotopically transplanted into Lewis rats. Under ketamine (Ketamin, 100 mg/kg intra-peritoneal injection; CP-Pharma, Burgdorf, Germany) and xylacine (Rompun, 10 mg/kg, peripheral injection; Bayer, Leverkusen, Germany) anaesthesia the left donor kidney was removed, cooled and positioned orthotopically into the recipient. Donor and recipient renal artery, vein, and ureter were anastomosed end-to-end with 10-0 Prolene sutures. No ureteral stent was used. To overcome infectious complications due to operation rats received cephtriaxone (Rocephin, 20 mg/kg/day, intramuscular injection, Hoffmann-la Roche AG, Grenzach-Wyhlen, Germany) on the first postoperative day. Animals were treated with low-dose Cyclosporine A (1.5 mg/kg/day, subcutaneous injection, Novartis GmbH, Nürnberg, Germany) during the first 10 days after transplantation to overcome an initial episode of acute rejection. The contralateral native kidney was removed on the 10th postoperative day**.**

3.3 Groups and treatment

The recipient animals received either everolimus (0.5mg/kg/day, Novartis S.A., Basel, Switzerland) dissolved in 5% glucose solution or vehicle (5% glucose solution) by daily gavage (9 animals per group). Animals were randomly assigned to the following groups after

transplantation: **EVR 12-20** = everolimus treatment from week 12 to 20; **EVR 12-28** = everolimus treatment from week 12 to 28; **EVR 20-28** = everolimus treatment from week 20 to 28; **VEH 12-20** = vehicle treatment from week 12 to 20; **VEH 12-28** = vehicle treatment from week 12 to 28. Animals from group EVR 12-20 and VEH 12-20 were sacrificed at week 20, while those from group EVR12-28, EVR 20-28 and VEH 20-28 were sacrificed at week 28.

3.4 Functional measurements

Every four weeks, 24-hour urine samples were collected using metabolic cages with a urine-cooling system. Quantitative urine protein was nephelometrically determined (28). Graft weight and body weight were measured at the end of the observation period.

3.5 Histology

Paraformaldehyde-fixed and paraffin embedded tissue sections were stained with Hematoxylin and Eosin (H. E.) to evaluate tubulointerstitial fibrosis, vasculopathy and tubular atrophy. Periodic acid schiff (PAS) reaction was performed to evaluate glomerulosclerosis. CAN was graded according to parameters adapted from the Banff´97 classification (38): 0 = no signs of CAN; grade 1 = mild CAN with mild fibrosis and tubular atrophy (affected 5-15% area of section), mild vasculopathy (intimal proliferation for luminal obstruction area affected 1-25% of one vessel) ; grade 2 = moderate CAN with moderate fibrosis and tubular atrophy(affected 16-50% area of section), moderate vasculopathy (luminal obstruction area affected 25-50% of one vessel); grade 3 = severe CAN with severe fibrosis and tubular atrophy (affected >50% area of section), severe vasculopathy (luminal obstruction area affected >50% of one vessel). Glomerulosclerosis was evaluated by counting all glomeruli of the section and calculate the percentage of sclerotic glomeruli.

3.6 Immunohistochemistry

3.6.1 Immunohistochemical staining for macrophage (ED1) and $CD5^+$ T cell (OX19) by alkaline phosphatase anti-alkaline phosphatase (APAAP)

Cellular infiltration was analyzed by immunohistochemistry studies. The procedure was performed on frozen sections (4μm) fixed in acetone. Sections were incubated with monoclonal mouse primary antibodies against ED1 and OX19 (Serotec, Oxford, United Kingdom) followed by incubation with a secondary rabbit anti-mouse antibody (Dako, Glostrup, Denmark) and development of the colour signal by an alkaline phosphatase anti-alkaline phosphatase (APAAP) complex (Dako, Glostrup, Denmark). Counterstaining was proceeded with Mayer's haemalaun (Merck, Darmstadt, Germany). ED1 and OX19 immunoreactive cells with cytoplasm stained in red were counted at 400 x magnification and presented as cells per field of view (cells/fv). At least 20 fields of view were observed. Negative control was performed in the same procedure except that sections were incubated with PBS instead of the primary antibody.

3.6.2 Immunohistochemical staining for proliferation cellular nuclear antigen (PCNA) by streptavidin-biotin conjugated peroxidase (ABC)

Proliferating cells were analyzed with ABC method. Graft tissue was fixed in 4% buffered formalin and embedded in paraffin. After sections (4μm) were dewaxed and hydrated, they were treated with 10mM citrate acid (Merck, Darmstadt, Germany) buffer (2.1g citrate acid monohydrate in 1000ml distilled water, pH 6.0), heated up in a high-pressure cooker for 15 minutes, cooled down slowly to room temperature for 30 minutes, and then dipped into 3% H_2O_2 (Roth, Karlsruhe, Germany) in distilled water for 30 minutes followed by blockade with the diluted ready- to- use normal horse serum (R.T.U. Vectastain Elite ABC-Peroxidase Universal Kit, Vector Laboratories, Burlingame, CA) for 20 minutes.

After incubation with the monoclonal mouse anti-human proliferation cellular nuclear antigen (PCNA, clone PC10, DAKO, Glostrup, Denmark) (1:50 diluted) for 1 hour at room temperature, sections were incubated with the diluted biotinylated universal secondary antibody and then with the vectastain ABC reagent (R.T.U. Vectastain Elite ABC-Peroxidase Universal Kit, Vector Laboratories, Burlingame, CA) for 30 minutes respectively. Thereafter the Peroxidase substrate 3, 3'-diaminobenzidine (DAB) (Vector Laboratories, Burlingame, CA) was applied to develop the positive colour and counterstained with Mayer's haemalaun (Merck, Darmstadt, Germany) was finally performed. Positive cells which nuclei stained in brown were counted and presented as cells per field of view (cells/fv). At least 20 fields of view per section or per specimen were evaluated at 400 x magnification. Negative control was performed in the same procedure except that sections were incubated with phosphate buffered saline (PBS, pH7.4) instead of the primary antibody.

3.7 Terminal deoxynucleotidyl transferase -mediated dUTP nick end labelling assay (TUNEL)

TUNEL was performed on frozen sections (4μm) fixed in 4% paraformaldehyde as described elsewhere (9). Briefly, sections were incubated with 0.1% Triton X-100 (Sigma, Munich, Germany) and 0.1% sodium citrate in phosphate buffered saline (PBS, pH7.4) at 4 °C for 2 minutes, washed in PBS and incubated with TUNEL mix solution containing terminal deoxynucleotidyl transferase (Boehringer Mannheim, Germany) and dUTP digoxigenin-labelled (Boehringer Mannheim, Germany) at 37°C for 90 minutes. Sections were then washed with stop/wash buffer (30mM Sodium citrate, 300mM sodium chloride in distilled water). After that they were incubated with the rabbit anti-digoxigenin antibody (Boehringer Mannheim, Germany) at 37°C for another 90 minutes. Antibody binding was visualized using Fast Red chromogen solution (DAKO, Glostrup, Denmark). Positive controls

were treated with DNase I (Boehringer Mannheim, Germany) and performed as described above. Negative controls were incubated with PBS instead of TUNEL mix solution. Sections were counterstained with Mayer's haemlaun (Merck, Darmstadt, Germany). All positive tubular epithelial cells which nuclei stained in red were counted at a 400x magnification and noted as cells per field of view (cells/fv).

3.8 Reverse transcription polymerase chain reaction (RT-PCR)

Total cellular RNA was isolated and transcribed into cDNA by reverse transcription as previously described (44). Specific cDNA products corresponding to the mRNA of TGF-β, PDGF-A and –B chain, and β-actin were amplified by polymerase chain reaction using their respective primers (PDGF-A sense: CACGGATCCAAGTATTGAGGAAGCCA; PDGF-B sense: GAAGCCAGTCTTCAAGAAGGCCAC; TGF-β sense: GGACTACTACGCCAAAGAAG; β-actin sense: CTATCGGCAATGAGCGGTTC). After gel electrophoresis, bands were stained with ethidium bromide and visualized by UV transillumination. For semiquantitative analysis, gels were digitized for computerized densitometry of specific bands. Data were expressed as ratio between the density of the specific product and that of the housekeeping gene (β-actin).

3.9 RNase protection assay (RPA)

Total RNA was extracted using Trizol reagent (Gibco, Karlsruhe, Germany) as described previously (40). Briefly, tissues were homogenized in 1ml Trizol, and then added 0.2ml chloroform (Merck, Darmstadt, Germany). After centrifugation for 15 minutes at 12,000 x g at 4°C, the upper aqueous phase was transferred into a new labelled tube and incubated with 0.5ml isopropyl alcohol (Merck, Darmstadt, Germany) for 10 minutes at room temperature. Then the samples were centrifuged again at 12,000 x g at 4°C for 10 minutes.

The supernatant was removed and pellets were mixed with 1ml 75% ethanol (Merck, Darmstadt, Germany). After centrifugation again at 7,500 x g for 5 minutes at room temperature, supernatant was carefully removed thoroughly and pellets were air dried for 18 minutes. Then pellets were dissolved in 10µl RNase free water and stored at -80°C for further detection. The quantification of the extracted RNA was preceded by the biophotometer (Eppendorf, Hamburg, Germany).

Intragraft mRNA expression of fasL, bcl-2, bax, caspase-1, caspase-3 and GAPDH (RiboQuant Multi-Probe template set, Pharmingen, Becton Dickinson GmbH, Hamburg, Germany) was determined by RNase protection assay using the In vitro Transcription Kit and RPA Kit (Pharmingen, Hamburg, Germany) as described previously (40). Briefly, ^{32}P-labeled antisense riboprobes were synthesized with the use of T7 RNA polymerase transcription in the presence of [α^{32}P]UTP. Radiolabelled antisense riboprobes were then hybridized with 10 µg of total RNA extracted from allograft at 56°C overnight. After hybridization, RNase A + T1 were added to digest unhybridized RNA and duplex RNA hybrids were separated by electrophoresis on a 5% polyacrylamide gel. Intensity of the protected bands was quantified by a phosphor imaging analyzer (Fuji-BAS 1500, Düsseldorf, Germany) and the ratios of the investigated mRNA to GAPDH (internal control) were calculated.

3.10 Statistical analysis

Data were expressed as mean ± standard error of mean (SEM), and compared using ANOVA, chi-square and Kruskal-Wallis test. Statistical significance was accepted at $p < 0.05$.

4. Results

4.1 Everolimus treatment improved proteinuria and decreased the progression of CAN

4.1.1 24-hour proteinuria

Treatment with everolimus initiated at week 12 (EVR 12-20; EVR 12-28), when changes of CAN became detectable in this model, resulted in a significantly decreased proteinuria as compared to controls at weeks 20 and 28 (VEH 12-20; VEH 12-28) ($p < 0.05$) (Table 1, Figure 2 and 3).

Surprisingly, everolimus reduced proteinuria even in animals with delayed treatment (from week 20), a time of histomorphologically apparent changes, although proteinuria was similar to controls before treatment was initiated (EVR 20-28 vs. VEH 12-28, $p = 0.03$) (Table 1, Figure 3). All animals survived the observation period.

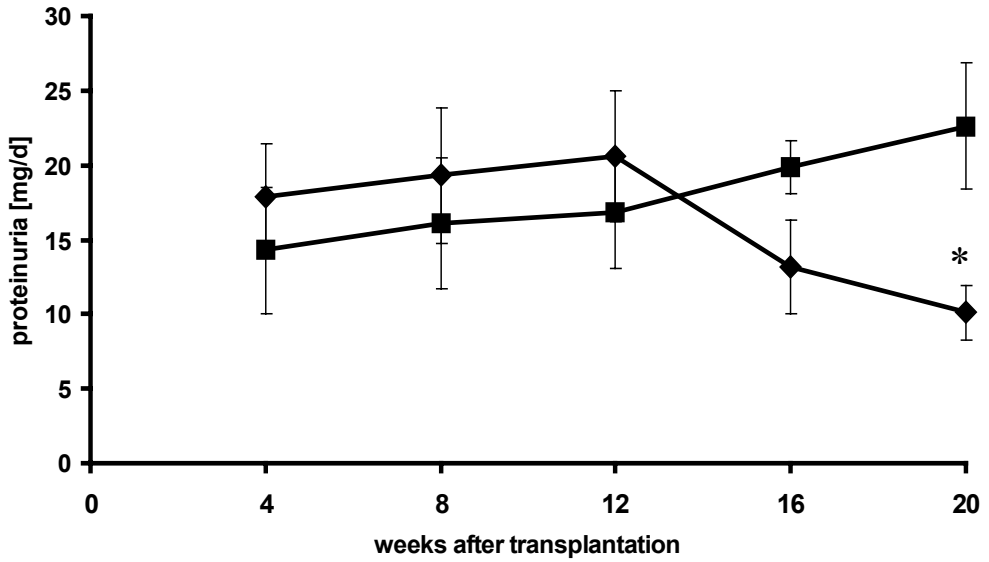

Figure 2. 24-hour urinary protein excretion of animals treated with everolimus from week 12 to 20 (EVR 12-20) (◆) and vehicle from week 12 to week 20 (VEH 12-20) (■) after transplantation. * Denoted $p<0.05$ while compared to the control group.

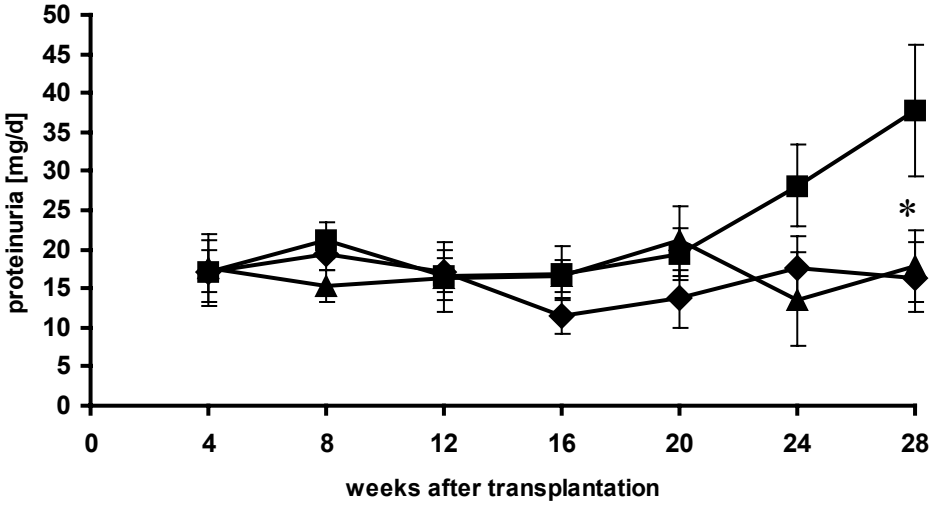

Figure 3. 24-hour urinary protein excretion of animals treated with everolimus from week 12 to week 28 (EVR 12-28) (◆), everolimus from week 20 to week 28 (EVR 20-28) (▲) and vehicle from week 12 to week 28 (VEH 12-28) (■) after transplantation. * Denoted $p<0.05$ while compared to the control groups.

4.1.2 Grade of CAN, glomerulosclerosis, and inflammatory infiltrates

4.1.2.1 Everolimus treatment decreased the progression of CAN

Glomerulosclerosis in everolimus treated animals was lower as compared to controls (EVR 12-20 vs. VEH 12-20, $p = 0.03$; EVR 12-28 vs. VEH 12-28, $p = 0.05$) (Figure 4). The grade of CAN was significantly ameliorated in everolimus treated animals as compared to controls (EVR 12-20 vs. VEH 12-20, $p = 0.032$; EVR 12-28 vs. VEH 12-28, $p = 0.001$) (Table1, Figure 5). Vasculopathy was basically absent in everolimus treated animals while controls had mild vasculopathy (Figure 5). However, even animals treated with vehicle up to week 28 developed only mild, in some cases moderate signs of vasculopathy in our model.

Infiltration of graft tissue by T-cells (OX19 positive) and macrophages (ED1 positive) tended to be lower in everolimus treated animals at 20 weeks than in controls (EVR 12-20 vs. VEH 12-20, $p = 0.07$) while treatment with everolimus from week 12 to 28 reduced T-cell and macrophage infiltration significantly (EVR 12-28 vs. VEH 12-28, $p < 0.05$) (Table 1).

4.1.2.2 Delayed treatment with everolimus also decreased grade of CAN

The grade of CAN was significantly lower in animals with delayed everolimus treatment as compared to controls (EVR 20-28 vs. VEH 12-28, p = 0.025) (Table 1, Figure 5).

In animals with delayed everolimus treatment glomerulosclerosis tended to reduce as compared to controls (EVR 20-28 vs. VEH 12-28, p = 0.17) (Figure 4), T-cell and macrophage infiltration and vasculopathy were lower and at the level of controls after 20 weeks (VEH 12-20) (Table 1, Figure 5).

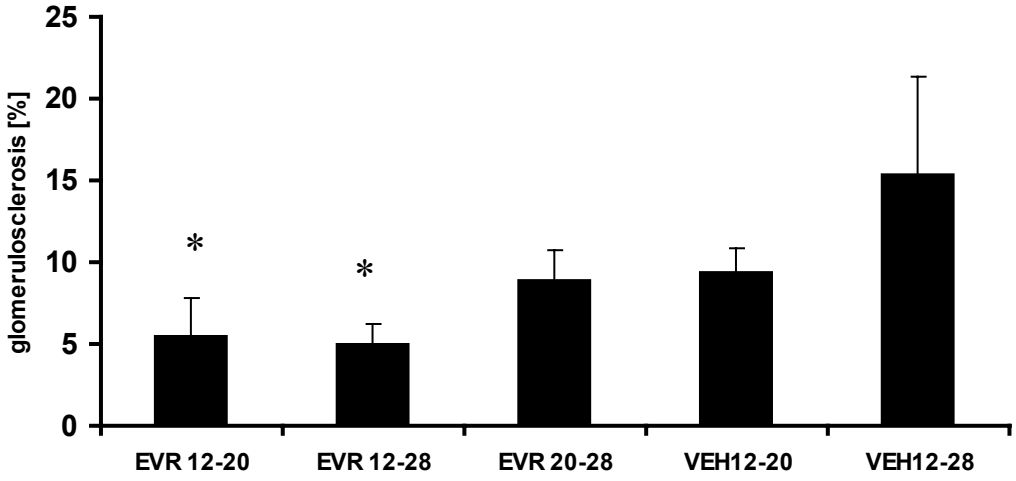

Figure 4. Glomerulosclerosis of graft tissue. Animals received everolimus treatment had a lower glomerulosclerosis as compared to controls after 20 or 28 weeks, respectively (EVR 12-20 vs. VEH 12-20 p = 0.03, and EVR 12-28 vs. VEH 12-28 p = 0.05). Even animals with delayed treatment had a lower glomerulosclerosis as compared to controls (EVR 20-28 vs. VEH 12-28, p = 0.17). * Denoted $p<0.05$ while compared to the control groups.

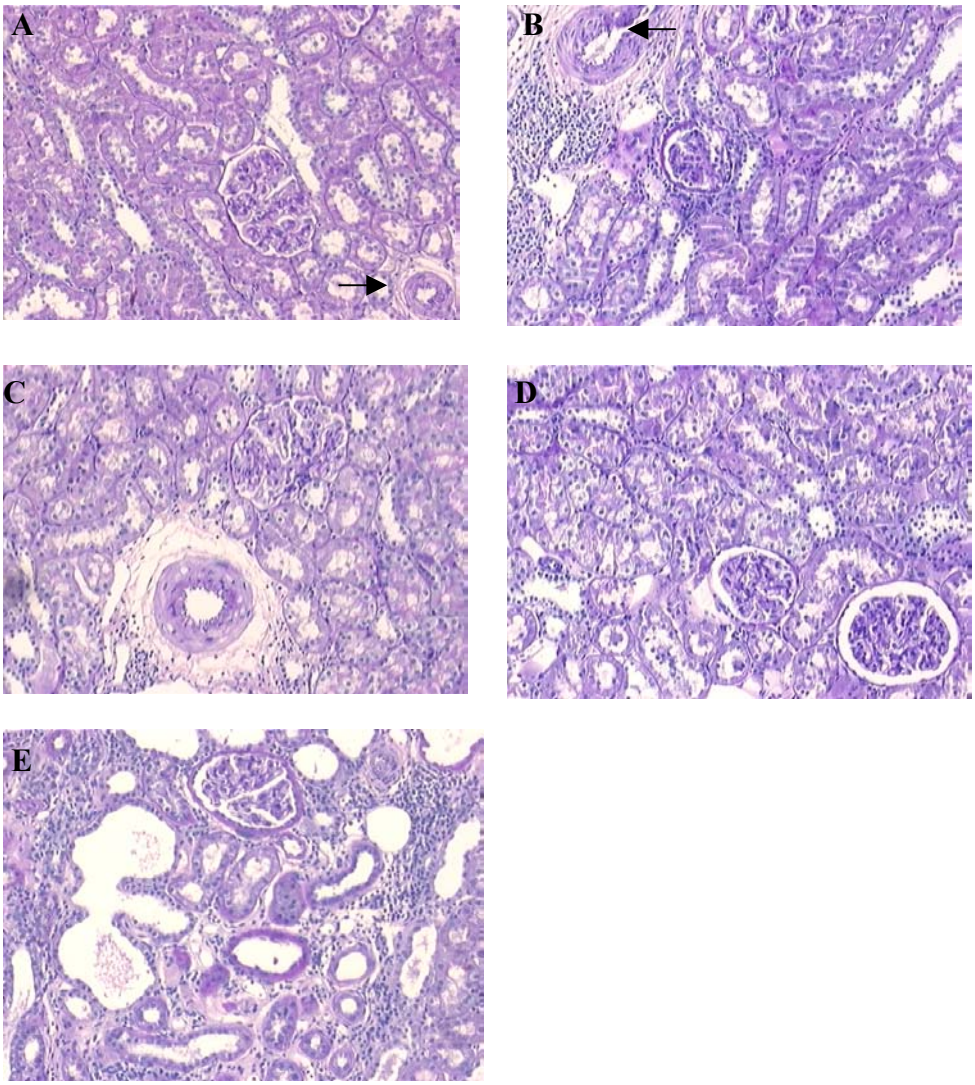

Figure 5. Histology of kidney grafts, PAS reaction, X 100. **(A)** Normal tubuli, glomeruli, and a regular artery (→) in animals treated with everolimus from week 12 to 20 (EVR 12-20); **(B)** Glomerulosclerosis, inflammatory infiltrates and discrete intimal hyperplasia (→) after 20 weeks in controls (VEH 12-20) ; **(C)** Normal glomeruli, mild tubular dilation/atrophy and normal artery after 28 weeks in animals treated with everolimus from week 12 to 28 (EVR 12-28) ; **(D)** Normal tubuli, mild tubular dilation / atrophy, normal glomeruli, and normal artery in animals treated with everolimus from week 20 to 28 (EVR 20-28); **(E)** Glomerulosclerosis, tubular atrophy, interstitial fibrosis, and vasculopathy after 28 weeks in controls (VEH 12-28).

4.2 Everolimus increased the number of apoptotic cells

The number of apoptotic cells was significantly higher in treated animals (EVR 12-20; EVR 12-28; EVR 20-28) as compared to controls (VEH 12-20; VEH 12-28) with the highest

number of almost exclusively tubular epithelial cells in animals with delayed everolimus treatment (EVR 20-28) ($p < 0.05$) (Table 1, Figure 6).

The number of proliferating cells did not significantly differ between the groups although animals treated with everolimus from week 12 to 28 tended towards higher numbers (Table 1, Figure 7).

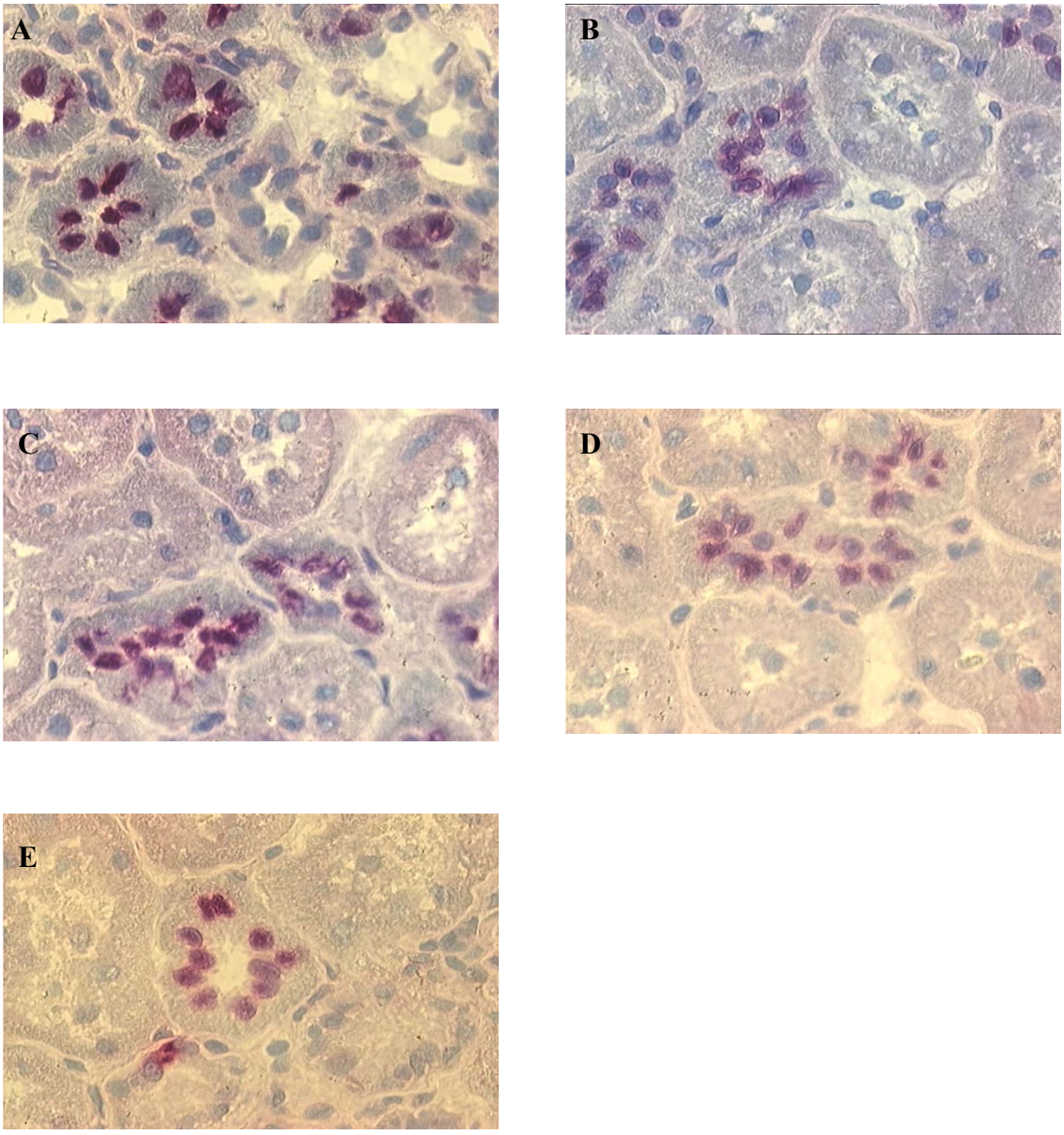

Figure 6. Apoptotic cells in allografts, TUNEL staining, X 400 (**A**) Marked increase of apoptosis cells in animals treated from week 20 to 28 (EVR 20-28); (**B**) Moderate increase of apoptotic cells in animals treated from week 12 to 28 (EVR 12-28); (**C**) Mild increase of apoptotic cells in animals treated from week 12 to 20 (EVR 12-20); (**D**) Apoptotic cells in control (VEH 12-28); (**E**) Apoptotic cells in control (VEH 12-20).

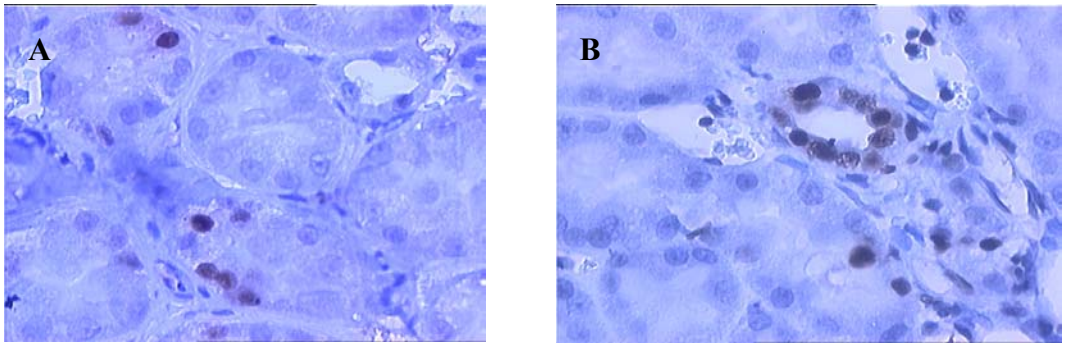

Figure 7. Cellular proliferation in allografts, PCNA immunohistochemistry staining, X 400. In comparison to controls (VEH 12-28) (**A**), everolimus treatment from week 12 to 28 (EVR 12-28) increased tubular proliferation (not significant) (**B**).

4.3 mRNA levels of apoptosis regulating factors

4.3.1 Ratio of bcl-2 / bax mRNA expression

The balance between bcl-2 mRNA and bax mRNA was shifted towards bax mRNA in animals with a treatment from week 20 to 28 (EVR 20-28) as compared to animals treated from week 12 to 28 (EVR 12-28) (Figure 8). The highest bcl-2/bax mRNA ratio was present in animals treated from week 12 to 20 (EVR 12-20) among the treated groups. Thus, pro-apoptotic Bax is favored in animals with delayed treatment. This was paralleled by the higher number of apoptotic cells in the group with delayed treatment (EVR 20-28). Controls had a balance favoring bcl-2 mRNA as compared to everolimus treated animals (VEH 12-28 vs. EVR 20-28, $p < 0.05$) (Figure 8).

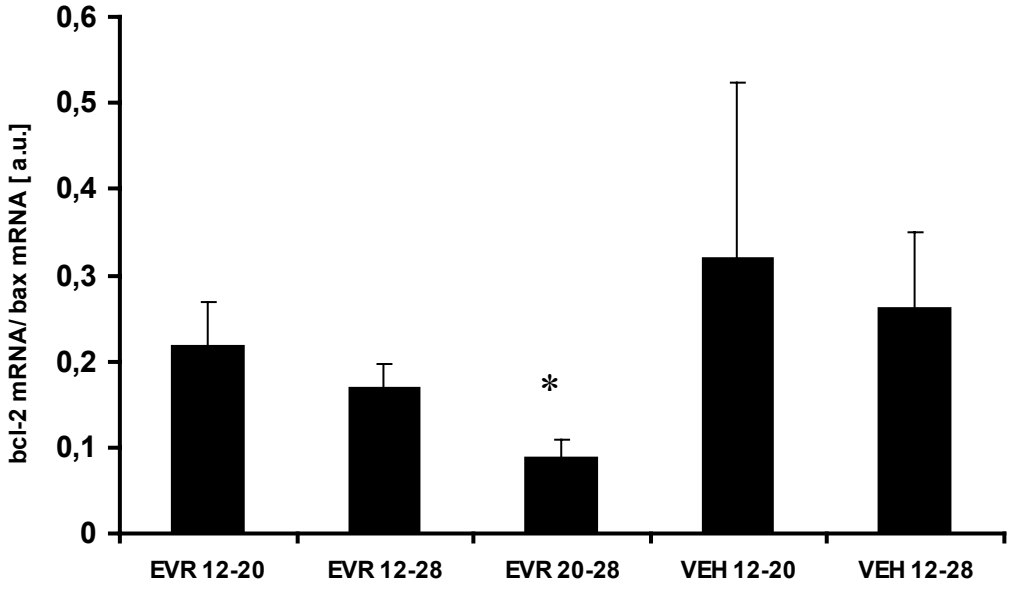

Figure 8. The balance between bcl-2 mRNA and bax mRNA was shifted towards bax mRNA from early treated animals (EVR 12-20) towards animals with delayed treatment (EVR 20-28) ($p = 0.03$). The balance was shifted more towards bcl-2 mRNA in controls as compared to everolimus treated animals (VEH 12-20, VEH 12-28).* Denoted $p<0.05$ while compared to the control group.

4.3.2 caspase-1 and caspase-3 mRNA expression

Caspase-1 and caspase-3 mRNA levels were increased in everolimus treated animals, the highest levels were at 28 weeks with delayed treatment (EVR 20-28) (EVR 12-20 vs. EVR 20-28, $p = 0.03$ for caspase-1 mRNA and $p = 0.001$ for caspase-3), while animals treated with everolimus from week 12 to 20 and 12 to 28 (EVR 12-20 and EVR 12-28) had similar levels as controls (VEH 12-20 and VEH 12-28). Levels were significantly higher in animals with delayed everolimus treatment as compared to controls (EVR 20-28 vs. VEH 12-28, $p = 0.04$ for caspase-1 mRNA and $p = 0.005$ for caspase-3) (Figure 9 and 10).

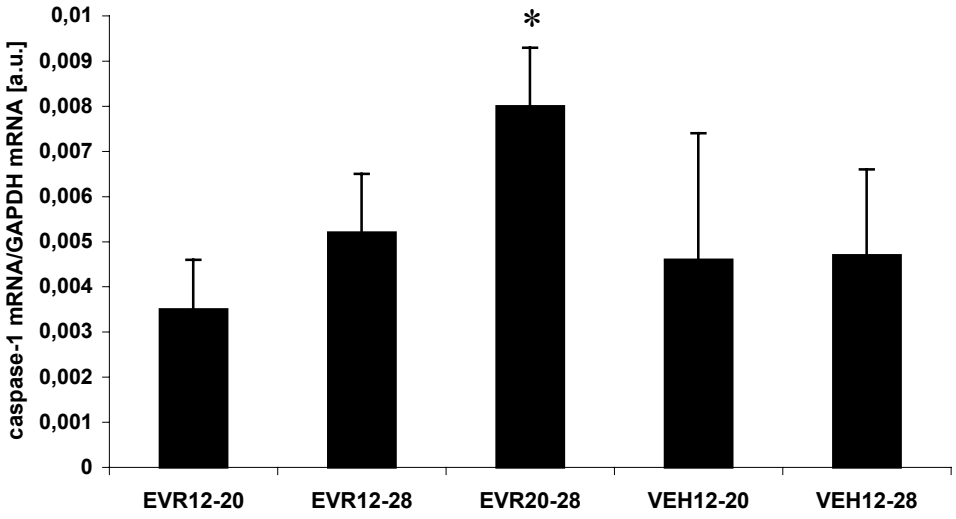

Figure 9. caspase-1/GAPDH mRNA levels in graft tissue. caspase-1 levels were increased in everolimus treated animals, the highest level was in animals with delayed treatment (EVR 12-20 vs. EVR 20-28, p = 0.03); controls had significantly lower levels as compared to animals with delayed treatment (VEH 12-28 vs. EVR 20-28, p = 0.04).* Denoted p<0.05 while compared to the control group.

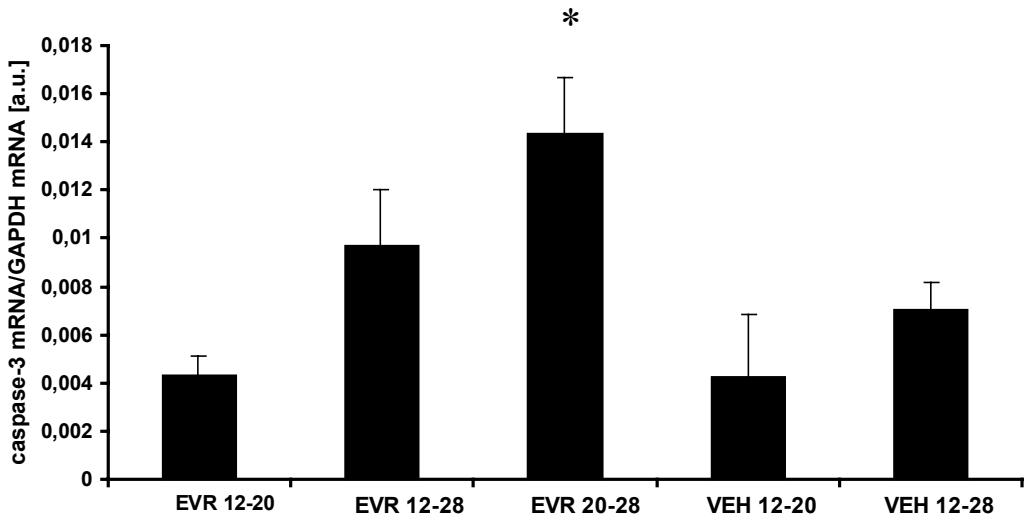

Figure 10. caspase-3/GAPDH mRNA levels in graft tissue. caspase 3 mRNA levels were increased in treated animals, the highest level was in animals with delayed treatment (EVR 12-20 vs. EVR 20-28, p = 0.001); controls had significantly lower levels than animals with delayed treatment (VEH 12-28 vs. EVR 20-28, p = 0.005). * Denoted p<0.05 while compared to the control group.

4.3.3 fasL mRNA expression

FasL mRNA levels were significantly higher in animals with delayed treatment (EVR 20-28) as compared to controls (EVR 20-28 vs. VEH 12-28, $p < 0.05$) (Figure 11).

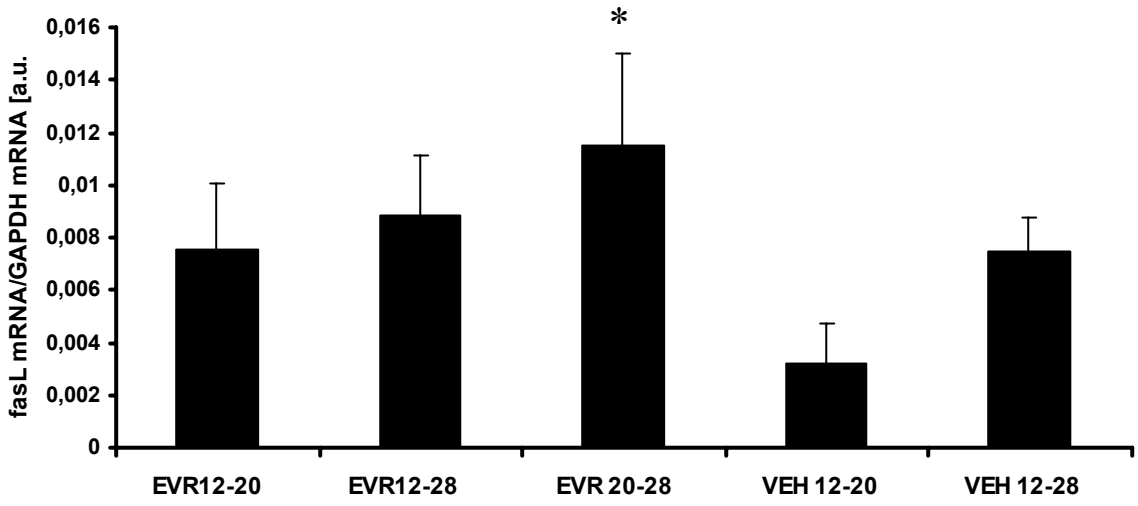

Figure 11. fasL/GAPDH mRNA levels in graft tissue. fasL mRNA levels were higher in animals with delayed treatment (EVR 20-28 vs. VEH12-28, $p < 0.05$). * Denoted $p<0.05$ while compared to the control group.

4.4 Growth factor mRNA

After 20 weeks TGF-β mRNA and PDGF-A levels were significantly lower in treated animals (EVR 12-20) than in controls (VEH 12-20) ($p < 0.05$) (Figure 12 and 13). Interestingly, TGF-β mRNA levels were significantly higher in animals treated until week 28 (EVR 12-28) rather than week 20 (EVR 12-20) ($p<0.05$) and tended to be higher than in controls (VEH 12-28) (Figure 12).

PDGF-A chain mRNA levels were also higher in animals treated with everolimus until week 28 (EVR 12-28) than up to week 20 (EVR 12-20) and were similar to controls at 28 weeks (VEH 12-28) (Figure13).

PDGF-B chain mRNA levels were similar in animals treated with everolimus from week 12 (EVR 12-20 and EVR 12-28) and controls (VEH 12-20; VEH 12-28) although they tended to be higher in animals with delayed everolimus treatment (EVR 20-28) (Figure 14).

TGF-β as well as PDGF-A and -B chain mRNA levels were highest in animals with delayed everolimus treatment (EVR 20-28) as compared to controls (VEH 12-28); this difference reached statistical significance for PDGF-A chain mRNA ($p < 0.05$) (Figures 12-14).

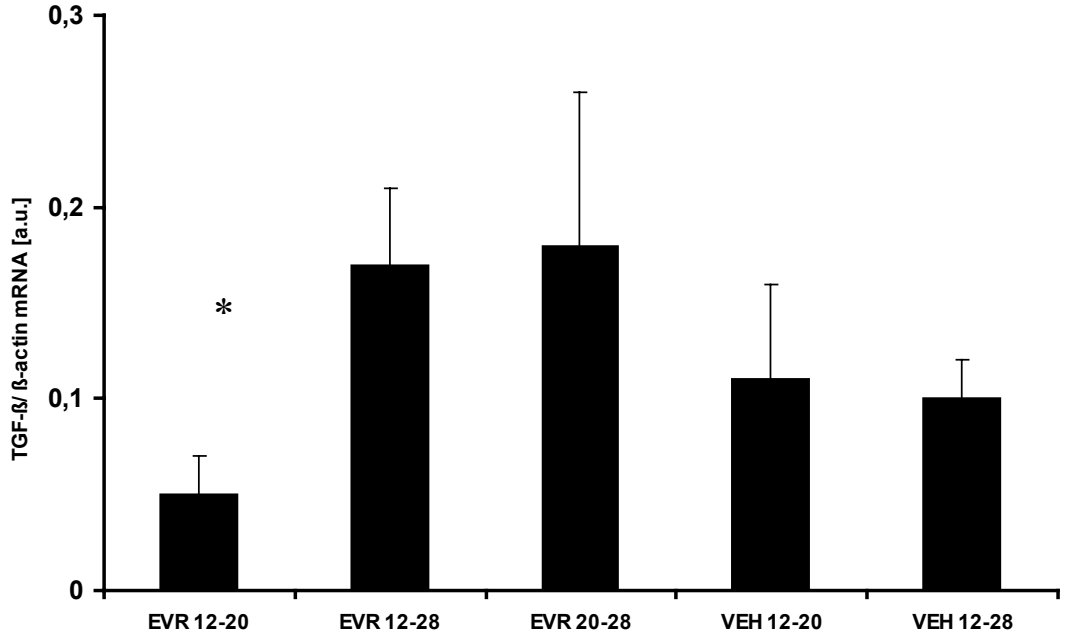

Figure 12. Ratio of TGF-β/β-actin mRNA levels in graft tissues. Everolimus treated animals (EVR 12-20) had significantly lower TGF-β mRNA levels than controls (VEH12-20) after 20 weeks ($p = 0.01$). However, TGF-β mRNA levels increased during follow-up in everolimus treated animals (EVR 12-28 and EVR 20-28) and tended to be higher in treated animals than in controls (VEH 12-28) (not significant).* Denoted $p<0.05$ while compared to the control group.

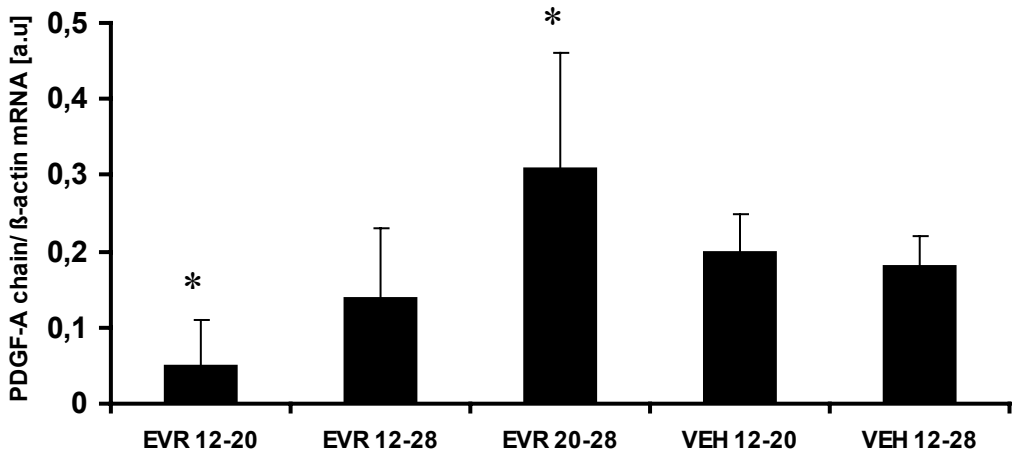

Figure 13. PDGF-A chain/β-actin mRNA levels in graft tissue. After 20 weeks, treated animals (EVR 12-20) had significantly lower PDGF-A chain mRNA levels than controls (VEH 12-20) ($p < 0.05$). PDGF-A chain mRNA levels increased in animals treated from week 12 and 20 up to week 28 (EVR 12-28 and EVR 20-28) with significantly higher levels in animals with a delayed treatment (EVR 20-28) as compared to controls (VEH 12-28) ($p = 0.04$). * Denoted $p<0.05$ while compared to the control group.

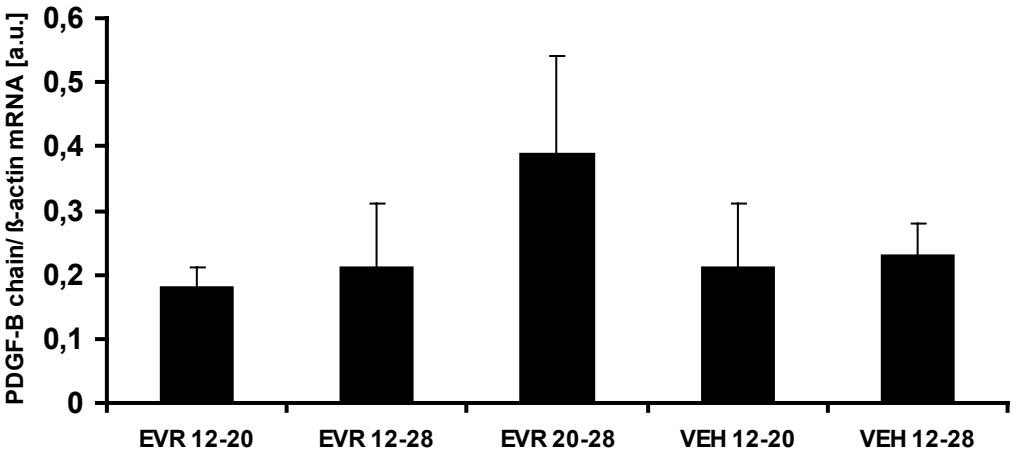

Figure 14. PDGF-B chain/β-actin mRNA levels in graft tissue. PDGF-B chain mRNA levels were increased in animals treated from week 12 and 20 up to week 28 (EVR 12-28 and EVR 20-28), respectively, with highest levels in animals with delayed everolimus treatment (EVR 20-28) as compared to controls (VEH 12-28) (not significant).

4.5 Other parameters

Graft weight / body weight ratio did not significantly differ between treated animals and controls (Table 1). Serum triglycerides were similar between experimental groups, serum cholesterol was significantly higher in treated animals (EVR 12-20, EVR 12-28, and EVR 20-28) as compared to controls (VEH 12-20 and VEH 12-28) ($p < 0.05$) (Table 1).

	EVR 12-20	EVR 12-28	EVR 20-28	VEH 12-20	VEH 12-28
24-hour proteinuria (mg/day)	10.1 ± 0.8 *	20.8 ± 3.4 *	17.8 ± 2.6 *	22.6 ± 2.4	37.8 ± 6.0
Graft weight/body weight	0.0036 ± 0.0002	0.0038 ± 0.0002	0.0037 ± 0.0005	0.004 ± 0.0003	0.004 ± 0.0004
Lipids					
Triglycerides (mg/dl)	56.6 ± 2.9	66.9 ± 3.7	66.3 ± 5.9	58.8 ± 9.2	65.4 ± 9.3
Cholesterol (mg/dl)	119.1 ± 7.6 *	134.0 ± 4.4 *	123.4 ± 4.1 *	84.0 ± 3.8	100.6 ± 3.9
Histology					
Grade of chronic allograft nephropathy (CAN) (n = number of cases):		p = 0.032	p = 0.001	p = 0.025	
No (CAN) (n)	5	7	0	0	0
Mild CAN (grade I) (n)	2	2	5	0	0
Moderate CAN (grade II) (n)	2	0	4	3	6
Severe CAN (grade III) (n)	0	0	0	2	2
Apoptotic cells (cells/ field of view)	20.1 ± 2.01 *	20.7 ± 0.98 *	24.8 ± 1.79 *	14.8 ± 2.51	11.5 ± 2.37
Proliferating cells (cells/view field)	4.09 ± 1.12	9.65 ± 2.03	4.8 ± 0.61	6.98 ± 1.07	4.93 ± 0.99
Cellular infiltration of the graft					
Macrophages (ED-1) (cells/field of view)	11.0 ± 1.25	13.6 ± 1.5 *	20.4 ± 2.0	15.2 ± 1.97	23.9 ± 3.4
Lymphocytes (OX-19) (cells/field of view)	9.9 ± 1.99	12.5 ± 1.2 *	21.7 ± 2.4	16.2 ± 2.13	24.5 ± 5.4

Table 1. Functional, histological, and immunohistological data. 24-hour protein excretion (at weeks 20 or 28 after transplantation as defined by the end of the observation period), graft/body weight ratio, lipid serum concentrations, immunocytochemistry, and histology data of the experimental groups at the end of the experiment. Data were given as mean ± SEM; * = EVR groups vs. VEH groups $p < 0.05$.

5. Discussion

5.1 Everolimus ameliorated CAN

Everolimus reduced the pace of CAN in the present study. These observations are in accordance with previous findings in models of aortic- or kidney transplantation (16) as well as in experiments of alloantigen independent vascular remodeling (17). However, all previous experiments focused on prevention rather than treatment.

Here we demonstrated for the first time that it is possible to reduce the pace of CAN even at an advanced stage. Animals that received early treatment with everolimus from week 12 after transplantation onwards developed a significantly lower proteinuria and a lesser degree of CAN in combination with significantly reduced glomerulosclerosis. After 28 weeks, inflammatory infiltrates were significantly lower in everolimus treated animals. Moreover, in animals with delayed everolimus treatment (from week 20 to 28), proteinuria significantly declined from values similar to controls to values comparable to those of the early treatment groups. These findings were paralleled by a significantly lower grade of CAN, lower glomerulosclerosis, and a trend towards lower inflammatory infiltrates.

These results, even present in the delayed treatment group after 28 weeks, a time when CAN was manifest and ongoing as documented by control animals, suggest that the morphological changes of CAN as well as the functional alterations observed after 20 weeks, at least in this experimental setting, can be maintained at a constant level and may even be partially reversible.

5.2 Everolimus and apoptosis in CAN

Everolimus might induce apoptosis of activated tubular cells. Activation of a cell is the result of stimuli (i.e. inflammation) that induce the expression of receptors regulating inflammation and the secretion of inflammatory mediators. Graft function could be prolonged as apoptosis of activated cells results in the elimination of cells that would otherwise

perpetuate chronic inflammatory processes, a feature of CAN. For rapamycin, such effects have been reported for rheumatoid synovial cells in which it decreased Bcl-2 and induced apoptosis (33). Furthermore, everolimus induced apoptosis in rhabdomyosarcoma cells (21) and enhanced apoptosis in a promyelocytic leukemia cell line in response to cisplatin (43).

Indeed, the number of apoptotic cells was elevated in everolimus treated animals, especially in those with delayed treatment. The ratio between bcl-2 mRNA, coding for the apoptosis-inhibiting Bcl-2, and bax mRNA, coding for the apoptosis-promoting Bax, was shifted towards apoptosis, particularly in animals with delayed treatment (EVR 20-28). Furthermore, the elevated levels of fasL- and caspase-3 mRNA correlated to the higher number of apoptotic tubular cells in animals with delayed everolimus treatment as well. The comparatively lower caspase 3 and bax mRNA levels in combination with the elevated bcl-2 mRNA levels in animals treated with everolimus from week 12 may result from a smaller number of activated cells and, thus, a reduced number of apoptotic cells. Altogether, the increased number of apoptotic cells and the shift towards pro-apoptotic factors in treated animals, particularly in those with delayed treatment may be caused by the higher number of activated cells that are prone to apoptosis.

In our experiments, predominantly tubular epithelial cells underwent apoptosis. These cells can produce collagens type I and III (27) and, thus, are important in the pathogenesis of interstitial fibrosis as well as the regulation of inflammatory processes.

The hypothesis was that everolimus could induce apoptosis of activated tubular cells, and eliminate these, in terms of the inflammatory response, dangerous cells from the graft. Tubular cells could then regenerate from the neighboring cells along the intact basal membrane. These findings of an apoptosis promoting effect of everolimus on tubular cells are paralleled by a recent report in a rat model of ischemia/reperfusion injury (10). Here, rapamycin impaired the recovery of renal function after ischemia/reperfusion due to an increased loss of tubular cells via apoptosis. As opposed to these results, apoptosis promoting

effect was analyzed at a time point shortly after the insult. The apoptosis promoting effects of rapamycin could result in tissue damage and deterioration of organ function during the acute phase after an insult, while it may resolve inflammation and remodeling during the late phase. This would also explain the increased rate of delayed graft function in kidney graft recipients treated with rapamycin shortly after transplantation (13). The deleterious effect of apoptosis during the acute phase after an insult is supported by the observation that inhibition of apoptosis reduced inflammation in a renal ischemia/reperfusion model (11). The effects of apoptosis are therefore likely to depend on the time point and the circumstances of its occurrence (11).

Interestingly, an increased number of apoptotic cells has been observed during chronic kidney (26) and heart rejection (24, 14, 51). This could be related to inflammatory processes in the graft as has been observed during renal ischemia/reperfusion (11). In this model everolimus could drive cells which are activated and, thus, perpetuate inflammation, into apoptosis. This would explain the increasing number of apoptotic cells from early to delayed treatment. Under those circumstances apoptosis would ameliorate chronic rejection and inflammation by the elimination of activated cells.

Caspase-1 is known to form the pro-inflammatory cytokines IL-1β and interlukin-18 (IL-18). In our experiments caspase-1 mRNA levels were significantly increased in animals with delayed everolimus treatment (EVR 20-28) as compared to levels of the other groups. Thus, the increased caspase-1 levels paralleled the number of apoptotic cells. Inhibition of caspase-1 has reduced inflammation and improved outcome in a model of cerebral ischemia/reperfusion (39). A broad spectrum caspase inhibitor also reduced inflammation in a model of renal ischemia/reperfusion (11), while absence of caspase-1 (knock out model) did not prevent ischemia/reperfusion injury (12). Thus, the role of caspase-1 in mediating inflammatory responses in the kidney may depend on time and type of injury.

The number of proliferating tubular epithelial cells did not significantly differ between everolimus treated animals and controls. A decreased number of proliferating cells has been observed in a rat model of acute renal failure after a short treatment with rapamycin (27). Whether everolimus or rapamycin have different effects on proliferation depending on the time point and the type of the insult remains to be investigated.

5.3 Everolimus and growth factor mRNA

TGF-β and PDGF, whose dimeric homo- or heteromer consists of an A- and/or a B-chain, play an important role in fibrogenesis during CAN. Growth factor mRNA levels increased from week 20 to week 28 in grafts of everolimus treated animals while they were significantly reduced (TGF-β and PDGF-A) in everolimus treated animals as compared to controls after 20 weeks. It was previously reported that everolimus reduced growth factor mRNA levels after transplantation in the Fisher to Lewis model (47). Those results do not directly reflect the current results as everolimus was administered in the earlier experiments over the entire observation period. Moreover, the observation period of 24 weeks in the former experiments might have been too short to detect an increase which now occurred after 28 weeks. Another group reported a reduction of growth factor mRNA by rapamycin only at very high doses (6 mg/kg/day) (17), doses much higher than those used in our experiments (0.5 mg/kg/d). The increased TGF-β- and PDGF mRNA levels in the everolimus treated animals may result from an inhibition of the intracellular signal transduction of growth factor receptors leading to a stimulation of the synthesis of growth factors.

5.4 Other functional parameters

Elevated cholesterol and triglyceride levels have been observed during the administration of rapamycin (5). In the present study, we observed elevated cholesterol levels as compared to

non-treated controls while triglyceride levels were similar. In our setting, everolimus did not affect hematocrit, creatinine clearance, or graft weight/body weight ratio.

5.5 Conclusion

In summary, our results suggested that everolimus could have the capacity to ameliorate CAN even at advanced stages. This could be explained by an induction of apoptosis in activated cells and, thus, the amelioration of intra-graft inflammation and remodeling. We conclude that everolimus is a promising tool for the prolongation of renal allograft survival.

6. Summary

Background: Chronic allograft nephropathy (CAN) is responsible for most cases of late kidney allograft loss. However, no effective treatment is available so far. Everolimus [40-O (2-hydroxyethyl) rapamycin] is a new immunosuppressive agent with anti-proliferative and apoptosis-enhancing effects. The present study investigated whether everolimus can ameliorate CAN even at advanced stages; whether everolimus treatment affects the level of growth factor mRNA, and/or the number of apoptotic cells in the graft.

Methods: Kidneys were transplanted from Fisher into Lewis rats and treated recipients with everolimus over different time periods. Grafts were analyzed 20 or 28 weeks after transplantation.

Results: Everolimus delayed the progression of CAN when started at an early stage. Surprisingly, everolimus even ameliorated CAN when initiated at an advanced stage. Interestingly, apoptosis was more prevalent in treated animals, particularly in those with delayed treatment as compared to controls.

Conclusions: In summary, everolimus ameliorates CAN as a result of anti-proliferative and/or apoptosis enhancing effects.

7. References

1. Adams, J.M., Corry, S.

   The Bcl-2 protein family: arbiters of cell survive.

   Science. 281(1998)1322-1326

2. Alnemri, E.S., Livingston, D.J., Nicholson, D.W., Salvesen, G., Thornberry, N.A., Wong, W.W., Yuan, J.

   Human ICE/CED-3 protease nomenclature.

   Cell. 87(1996)171

3. Ashkenazi, A., Dixit, V.M.

   Death receptors: signalling a modulation.

   Science. 281(1998)1305-1308

4. Bohler, T., Waiser, J., Budde, K., Lichter, S., Jauho, A., Fritsche, L., Korn, A.

   The in vivo effect of rapamycin derivative SDZ RAD on lymphocyte proliferation.

   Transplant. Proc. 30(1998)2195-2197

5. Brattstrom, C., Wilczek, H., Tyden, G., Bottiger, Y., Sawe, J., Groth, C.G.

   Hyperlipidemia in renal transplant recipients treated with sirolimus (rapamycin).

   Transplantation. 65(1998)1272-1274

6. Burns, A.T., Davies, D.R., McLaren, A.J., Cerundolo, L., Morris, P.J., Fuggle, S.V.

   Apoptosis in ischemia/reperfusion injury of human renal allografts.

   Transplantation. 66(1998)872-876

7. Cohen, G.M., Sun, X.M., Feamhead, H., MacFarlane, M., Brown, D.G., Snowden, R.T., Disdale, D.

   Formation of large molecular weight fragments of DNA is a key committed step of apoptosis in thymocytes.

   J. Immunol. 153(1994)507-516

8. Cummings, M.C.

Increased p53 mRNA expression in liver and kidney apoptosis.

Biochim. Biophys. Acta. 1315(1996)100-104

9. Cursio, R., Gugenheim, J., Ricci, J.E., Crenesse, D., Rostagno, P., Maulon, L., Saint-Paul, M.C., Ferrua, B., Auberger, A.P.

   A caspase inhibitor fully protects rats against lethal normothermic liver ischemia by inhibition of liver apoptosis.

   FASEB. J. 13(1999)253-261

10. Daemen, A.R.C., van't Veer, C., Denecker, G., Heemskerk, V.H., Wolfs, T.G.A.M., Clauss, M., Vandenabeele, P., Buurman, W.A.

    Inhibition of apoptosis induced by ischemia-reperfusion prevents inflammation.

    J Clin Invest. 104(1999)541-549

11. Daemen, M.A., de Vries, B., Buurman, W.A.

    Apoptosis and inflammation in renal reperfusion injury.

    Transplantation. 73(2002)1693-1700

12. Daemen, M.A.R.C., Denecker, G., van't Veer, C., Wolfs, T.G.A.M., Veandenabeele, P., Buurman, W.A.

    Activated caspase-1 is not a central mediator of inflammation in the course of ischemia-reperfusion.

    Transplantation. 71(2001)778-784

13. Davis, C.L., Marsh, C.L., Smith, K., Pollisar, N., Wrenshall, L.

    Rapamycin (RAPA) increases delayed graft function (DGF) following renal transplantation.

    J Am Soc Nephrol. 13(2002) 74P (Abstract)

14. Dong, C., Granville, D.J., Tuffnel, C.E., Kenyon, J., English, D., Wilson, J.E., McManus, B.M.

    Bax and apoptosis in acute and chronic rejection of rat cardiac allografts.

Lab Invest. 79(1999)1643-1653

15. Green P.R.

Apoptotic pathways: the road to run.

Cell. 94(1998)695-698

16. Geerling, R.A., de Bruin, R.W.F., Scheringa, M., Bonthuis, F., Jeekel, J., Ijzermans, J.N., Marquet, R.L.

Suppression of acute rejection prevents graft arteriosclerosis after allogenic aorta transplantation in the rat.

Transplantation.58 (1994)1258-1263

17. Gregory, C.R., Huie, P., Billingham, M.E., Morris, R.E.

Rapamycin inhibits arterial intimal thickening caused by both alloimmune and mechanical injury.

Transplantation. 55(1993)1409-1418

18. Hall, A.V., Jevnikar, A.M.

Significance of endothelial cell survival programs for renal transplantation.

Am. J. Kidney Dis. 14(2003)1140-1154

19. Hanbitz, M., Brunkhorst, R.

Influence of a novel rapamycin analogue SDZ RAD on endothelial tissue factor and adhesion molecule expression.

Transplant. proc. 34(2002)1124-1126

20. Hancock, W.H., Whitley, W.D., Tullius, S.G., Heemann, U.W., Wasowska, B., Baldwin, W.M. 3rd, Tilney, N.L.

Cytokines adhesion molecules and the pathogenesis of chronic rejection of rat renal allografts.

Transplantation. 56(1993)643-650

21. Hosoi, H., Dilling, M.B., Schikata, T., Liu, L.N., Shu, L., Ashmun, R.A., Germain, G.S., Abraham, R.T., Houghton, P.J.
Rapamycin causes poorly reversible inhibition of mTOR and induces p53-independent apoptosis in human rhabdomyosarcoma cells.
Cancer Res. 59(1999)886-894

22. Irmler, M., Steiner, V., Ruegg, C., Wajant, H., Tschopp, J.
Caspase-induced inactivation of the anti-apoptotic TRAF1 during Fas ligand-mediated apoptosis.
FEBS Lett. 25(2000)129-133

23. Junaid, A., Kren, S.M., Rosemberg, M.E., Nath, K.A., Hostetter, T.H.
Physiological and structural responses to chronic experimental renal allograft injury.
Am. J. Physiol. 267(1994)F1102-1106

24. Koglin, J., Russell, M.E.
Alloimmune-mediated apoptosis. Comparison in mouse models of acute and chronic cardiac rejection.
Transplantation. 67(1999)904-909

25. Kunikata, S., Nagano, T., Nishioka, T., Akiyama, T., Kurita, T.
Immunosuppressive action of FTY720 for renal allograft in a rat model.
Transplant. Proc. 31(1999)1157-1159

26. Laine, J., Etelamaki, P., Holmberg, C., Dunkel, L.
Apoptotic cell death in human chronic renal allograft rejection.
Transplantation. 63(1997)101-105

27. Lieberthal, W., Fuhro, R., Andry, C., Rennke, H., Abernathy, V.E., Koh, J.S., Valeri, R., Levine, J.S.
Rapamycin impairs recovery from acute renal failure: role of cell-cycle arrest and apoptosis of tubular cells.

Am J Physiol Renal Physiol. 281(2002) F693-F706

28. Liu, S., Lutz, J., Antus, B., Yao, Y., Baik, S., Illies, F., Heemann, U.
Recipient age and weight affect chronic renal allograft rejection in rats.
J. Am. Soc. Nephrol. 12(2001)1742-1749

29. Liu, X., Zou, H., Slaughter, C., Wang, X.
DFF, a heterodimeric protein that functions downstream of caspase-3 to trigger DNA fragmentation during apoptosis.
Cell. 89(1997)175-184

30. Martin, S.J., Finucane, D.M., Amarante-Mendes, G. P., O'Brien, G.A., Green, D.R.
Phosphatidylserine externalization during CD95-induced apoptosis of cells and cytoplasts requires ICE/CED-3 protease activity.
J. Biol. Chem. 271(1996)28753-28756

31. Martin S.J., Green, D.R.
Protease activation during apoptosis: death by a thousand cuts?
Cell. 82(1995)349-352

32. Martin, S.J., Reutelingsperger, C.P., McGahon, A.J., Rader, J.A., van Schie, R.C., LaFace, D.M., Green, D.R.
Early redistribution of plasma membrane phophatidylserine is a general feature of apoptosis regardless of the initiating stimulus: inhibition by overexpression of Bcl-2 and Abl.
J. Exp. Med. 182(1995)1545-1556

33. Migita, K., Eguchi, K., Ichinose, Y., Kawabe, Y., Tsukada, T., Aoyagi, T., Nagataki, S.
Effects of rapamycin on apoptosis of rheumatoid synovial cells.
Clin. Exp. Immunol. 108(1997)199-203

34. Nakopoulou, L., Stefanaki, K., Papadakis, Boletis, J., Zeis, P.M., Kostakis, A., Vosnides, G.
Expression of bcl-2 oncoprotein in various types of glomerulonephritis and renal allografts.
Nephrol. Dial. Transplant. 11(1996)997-1002

35. Nicholson, D.W., Thornberry, N.A.
Caspases: killer proteases.
Trends Biochem. Sci. 22(1997)229-306

36. Paolo, M., Alessandro, A.
Apoptosis: potential role in renal diseases.
Nephro. Dia. Transpl. 13(1998)1936-1943

37. Pual, L.C.
Dialysis and transplantation.
Curr. Opin. Nephrol. Hypertens. 8(1999)665-668

38. Racusen, L.C., Solez, K., Colvin, R.B., Colvin, R.B., Bonsib, S.M., Castro, M.C., Cavallo, T., Croker, B.P., Demetris, A.J., Drachenbery, C.B., Fogo, A. B., Furness, P., Gaber, L.W., Gibson, I.W., Glotz, D., Goldberg, J.C., Grande, J., Halloran, P.F., Hansen, H.E., Hartley, B., Hairy, P.J., Hill, C.M., Hoffman, E.O., Hunsicker, L.G., Lindblad, A.S., Yamaguchi, Y.
The Banff 97 working classification of renal allograft pathology.
Kidney Int. 55(1999)713-723

39. Rabuffetti, M., Sciorati, C., Tarozzo, G., Clementi, E., Manfredi, A.A., Beltramo, M.
Inhibition of caspase-1 activity by Ac-Tyr-Val-Ala-Asp-chloromethyl ketone induces long-lasting neuroprotectionin cerebral ischemia through apoptosis reduction and decrease of proinflammatory cytokines.
J Neuroscience. 20(2000)4398-4404

40. Refaeli, Y., Van Parijs, Y., London, C., Tschopp, J., Abbas, A.K.
Biochemical mechanisms of IL-2-regulated Fas-mediated T cell apoptosis.
Immunity. 8(1998)615-623

41. Schuler, W., Sedrani, R., Cottens, S., Haberlin, B., Schulz, M., Schuurman, H.J., Zenke, G., Zerwes, H.G., Schreier, M.H.
SDZ RAD, a new rapamycin derivative: pharmacological properties in vitro and in vivo.
Transplantation. 64(1997)36-42

42. Sehgal, S.N.
Rapamume (Sirolimus, rapamycin): an overview and mechanism of action.
Ther. Drug. Monti. 17(1995)660-665

43. Shi, Y., Frankel, A., Radvanyi, L.G., Penn, L.Z., Miller, R.G., Mills, G.B.
Rapamycin enhances apoptosis and increases sensitivity to cisplatin in vitro.
Cancer Res. 55(1995)1982-1988

44. Szabo, A., Lutz, J., Schleimer, K., Antus, B., Hamar, P., Philipp, T., Heemann, U.
Effect of angiotensin-converting enzyme inhibition on growth factor mRNA in chronic renal allograft rejection in the rat.
Kidney Intl. 57(2000)982-991

45. Terasaki, P.I., Cecka, J.M., Gjertson, D.W.
Current world opinion regarding the use of living donors.
Clin. Transpl.3 (1994)341-343

46. Viclicky, O., Müller, V., Zou, H., Szaobo, A., Vitko, S., Heemann, U.
RAD reduced compenstory renal graft hypertrophy in a rat model of chronic rejection.
Transplant. proc. 33(2001)2320-2321

47. Viklicky, O., Zou, H., Müller, V., Lacha, J., Szabo, A., Heemann, U.
SDZ-RAD prevents manifestation of chronic rejection in rat renal allografts.

Transplantation 69(2000)497-502

48. Wada, T., Schwarting, A., Kinoshita, K., Naito, T., Griffiths, R.C., Coffman, T.M., Kelly, V.R.

Fas on renal parenchymal cells does not promote autoimmune nephritis in MRL mice.

Kidney Int. 55(1999)841-851

49. Wajant, H.

The Fas signalling pathway: more than a paradigm.

Science. 269(2002)1635

50. Wever, P.C., Aten, J., Rentenaar, R.J., Hack, C.E., Koopman, G., Weening, J.J., Berge, I.J.

Apoptosis tubular cell death during acute renal allograft rejection.

Clin. Nephrol. 49(1998)28-34

51. Xu, B., Sakkas, L.I., Slachta, C.A., Goldman, B.I., Jeevanandam, V., Oleszak, E.L., Platsoucas, C.D.

Apoptosis in chronic rejection of human cardiac allografts.

Transplantation. 71(2001)1137-1146

52. Zimmermann, K.C., Green, D. R.

How cells die: apoptosis pathways.

J. Allergy Clin. Immunol. 108(2001) S99-103

53. Zou, H., Henzel, W.J., Liu, X., Lutschg, A., Wang, X.

Apaf-1 a human protein homologous to C. elegans CED-4 participates in cytochrome C-dependent activation of Caspase-3.

Cell. 90(1997) 405-413

8. Acknowledgments

Many thanks are owed to my tutor, Univ.- Prof. Dr. med. Uwe Heemann for his patience, encouragement, understanding and guidance. Without his support and open mind, I could not have accomplished this work successfully.

I would like to give my thanks to Dr. med. Jens Lutz for his encouragement, support and warm-hearted help. Many thanks go to Dr. med. Minghui Wang, Dr. med. Shanying Liu, Nengtai Ouyang and Eva Baumgartner for their extraordinary contributions to this work. Additional thanks to Ms. Magdalene Vogelsang for her organizational skills.